

Determination of photon PDF from High Mass Drell Yan data at LHC

F. Giulli and The xFitter Collaboration: V. Berone, A. Cooper-Sarkar,
A. Glazov, R. Placakyte, V. Radescu, J. Rojo, A. Saponov, etc.
(Dated: November 24, 2016)

abstract goes here: ...

CONTENTS

| | |
|----------------|---|
| I Introduction | 1 |
| II Theory | 1 |
| III Results | 1 |
| A Sensitivity | 1 |
| B PDF Fits | 2 |
| IV Conclusions | 2 |
| References | 2 |

I. INTRODUCTION

II. THEORY

Two processes contribute to opposite sign, same family, dilepton production at the LHC: the Drell-Yan quark-antiquark process and the photon-induced process. Both the contributions can be simulated with MadGraph5_aMC@NLO (version 2.4.3) and interfaced to APPLgrid (version 01-04-70) and aMCfast (version 01-03-00). A special release of APPLgrid is used to account for the photon PDF within the proton *need references for the programmes*. Both contributions are generated in the 5-flavour scheme, where all the quarks, except for the *top* quark, are treated as massless quarks; all the calculations are performed at fixed-order (FO) without parton showers.

Theoretical predictions for both the one-dimensional $\frac{d\sigma}{dm_{ll}}$ distribution (where m_{ll} is the invariant mass of the dilepton pair in the final state) and the double-differential distributions $\frac{d^2\sigma}{dm_{ll}d|y_{ll}|}$ (where $|y_{ll}|$ is the rapidity of the dilepton pair) and $\frac{d^2\sigma}{dm_{ll}\Delta\eta_{ll}}$ (where $\Delta\eta_{ll}$ represents the difference in pseudorapidity between the two leptons) are generated for both the electron and the muon channels.

These predictions are generated using the same selections as in reference [?] as follows:

- the invariant mass of the lepton pair is required to be greater than 116 GeV;
- the absolute value of the pseudorapidity of each lepton is required to be less than 2.5;
- the transverse momentum (p_T) of the leading lepton has to be greater than 40 GeV;

- the p_T of the sub-leading lepton has to be greater than 30 GeV.

The binning used is the same as used in reference [?]. For the invariant mass distribution, there are 12 bins between 116 GeV and 1.5 TeV with variable bin widths; and for both of the two-dimensional distributions, there are five different histograms, each one for a different invariant mass range: (a) $116 \text{ GeV} < m_{ll} < 150 \text{ GeV}$; (b) $150 \text{ GeV} < m_{ll} < 200 \text{ GeV}$; (c) $200 \text{ GeV} < m_{ll} < 300 \text{ GeV}$; (d) $300 \text{ GeV} < m_{ll} < 500 \text{ GeV}$; (e) $500 \text{ GeV} < m_{ll} < 1500 \text{ GeV}$. The APPLgrids for the first three m_{ll} intervals are divided into 12 bins with fixed bin width between $|y_{ll}^{min}|$ ($|\Delta\eta_{ll}| = 0.0$) and $|y_{ll}^{max}|$ ($|\Delta\eta_{ll}| = 2.4$), while the final two m_{ll} intervals are divided into 6 bins with fixed bin width scanning the same $|y_{ll}|$ and $|\Delta\eta_{ll}|$ ranges.

Dynamical renormalization (μ_R) and factorization (μ_F) scales are used in the calculations and both are set to m_{ll} . The theoretical calculations were validated by comparing both the NLO QCD + LO EW predictions and the LO PI predictions to those computed using the FEWZ 3.1 framework. These calculations are evaluated in the G_F electroweak scheme, with the following values for the couplings: $\alpha_S = 0.118$; $1/\alpha_{EW} = 1/127$. The difference between the two predictions is at most 1%, for both the 1-dimensional and the 2-dimensional distributions.

In order to make a next-to-next-to-leading order (NNLO) fit k -factors (k_F) are computed matching the NLO QCD + LO EW cross sections to higher order (HO) calculations. These are computed using FEWZ, with the same input parameters as for the NLO computations. The k_F are defined as:

$$k_F = \frac{NNLO \text{ QCD} + NLO \text{ EW} \sigma}{NLO \text{ QCD} + LO \text{ EW} \sigma} \quad (1)$$

The MMHT2014NNLO PDF set is used to compute both numerator and denominator. The k_F are close to the unity and their variation is $\sim 2\%$. *provide Table of Final k-factors?*

Discuss theory improvements: addition of the NLO QED+QCD piece

III. RESULTS

A. Sensitivity

show impact of HM DY on PDFs using sensitivity studies based on pseudo-data, for which we only use the data

uncertainties, while central value are fixed: HERA I+II vs HERA I+II + HMDY \rightarrow see the sensitivity plots from the previous email

conclusion: HMDY data has a large impact on photonPDF

B. PDF Fits

In order to make a full PDF fit the ATLAS Drell-Yan data data are fitted together with the final combined inclusive cross section data from HERA [?]. The HERA data provide information on the quark/antiquark and gluon content of the proton and the Drell-Yan data add information on the photon content of the proton. The NLO and NNLO pQCD predictions are fitted to the data using the xFitter open source pQCD fitting platform [?]. The DGLAP equations [?] are solved using the programme QCDNUM which has been modified to include the photon PDF in the proton [?]. The DGLAP equations yield the PDFs at all scales if they are input as functions of x at a starting scale Q_0^2 , which should be large enough that perturbative QCD can be assumed to be valid. For the present analysis this value is chosen to be $Q_0^2 = 7.5 \text{ GeV}^2$. This is also the value chosen for the minimum value of Q^2 for data entering the fit. The charm and beauty masses are chosen to be $m_c = 1.47 \text{ GeV}$ and $m_b = 4.5 \text{ GeV}$ following the HERA analysis. The value of $\alpha_s(M_Z)$ is chosen to be $\alpha_s(M_Z) = 0.118$ [?]. The value of Q_0^2 is above the charm mass squared, however a version of the programme is used which displaces the charm threshold from the charm mass [?] such that the threshold is at Q_0^2 . The form of the χ^2 used for the fit is that defined in the H1 paper [?]. Alternative forms have also been tried with no significant difference to our results.

The PDF parametrisation input at Q_0^2 is determined by the technique of saturation of the χ^2 [?]. The parametrised PDFs are the valence distributions xu_v and xd_v , the gluon distribution xg , and the u -type and d -type sea, $x\bar{U}$, $x\bar{D}$, where $x\bar{U} = x\bar{u}$ and $x\bar{D} = x\bar{d} + x\bar{s}$, and finally the photon distribution $x\gamma$. The following standard functional form is used to parametrise them:

$$xf(x) = Ax^B(1-x)^C(1+Dx+Ex^2) \quad (2)$$

where the normalisation parameters A_{u_v} , A_{d_v} and A_g are constrained by the number sum-rules and the momentum sum-rule, respectively. The B parameters $B_{\bar{U}}$ and $B_{\bar{D}}$ are set equal, such that there is a single B parameter for the sea distribution. The data are not sensitive to the strangeness content of the proton which is thus set such that $x\bar{s} = 0.5\bar{D}$, following the ATLAS analysis [?]. The further constraint $A_{\bar{U}} = 0.5A_{\bar{D}}$ is imposed such that $\bar{u} = x\bar{d}$ as $x \rightarrow 0$. The D and E parameters are introduced one by one until no significant improvement in χ^2 is found.

For the NNLO fit a $\chi^2/ndf = 1.18$, with a partial $\chi^2/ndp = 1.15$ for the high-mass Drell-yan data [up-

date with final numbers], is achieved for the following parametrisation, which has 11 parameters for the quarks and gluons and 5 parameters for the photon:

$$xu_v(x) = A_{u_v}x^{B_{u_v}}(1-x)^{C_{u_v}}(1+E_{u_v}x^2), \quad (3)$$

$$xd_v(x) = A_{d_v}x^{B_{d_v}}(1-x)^{C_{d_v}}, \quad (4)$$

$$x\bar{U}(x) = A_{\bar{U}}x^{B_{\bar{U}}}(1-x)^{C_{\bar{U}}}, \quad (5)$$

$$x\bar{D}(x) = A_{\bar{D}}x^{B_{\bar{D}}}(1-x)^{C_{\bar{D}}}, \quad (6)$$

$$xg(x) = A_gx^{B_g}(1-x)^{C_g}(1+E_gx^2), \quad (7)$$

$$x\gamma(x) = A_\gamma x^{B_\gamma}(1-x)^{C_\gamma}(1+D_\gamma x + E_\gamma x^2) \quad (8)$$

$$(9)$$

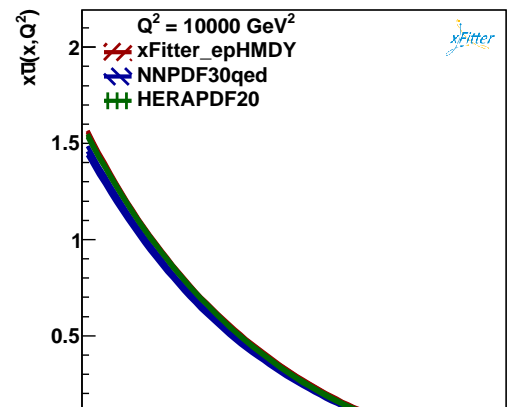
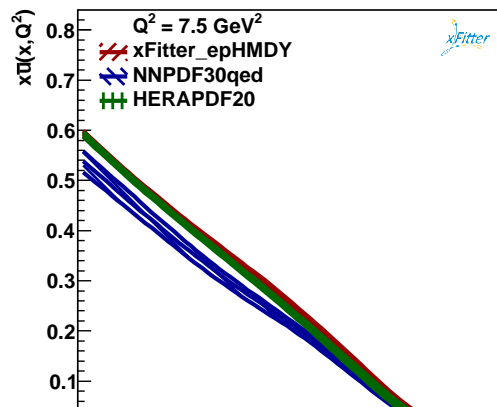
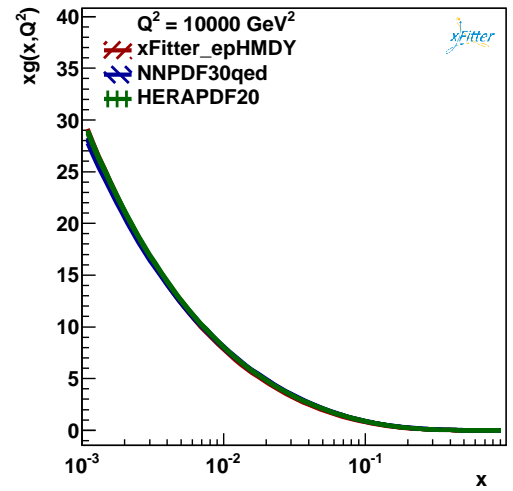
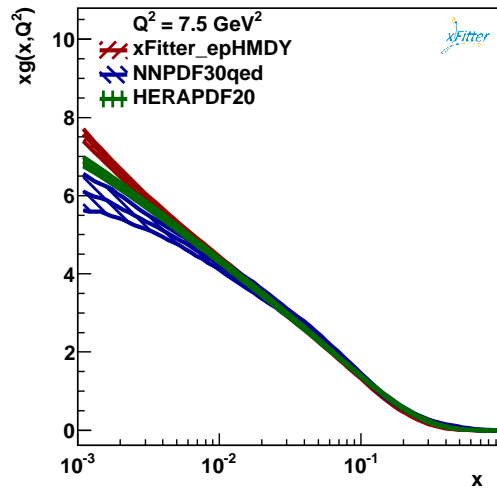
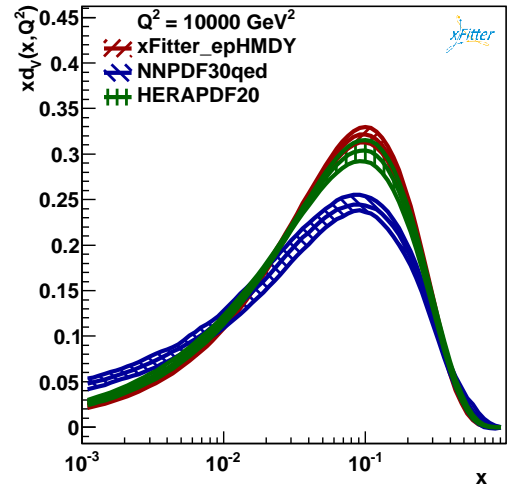
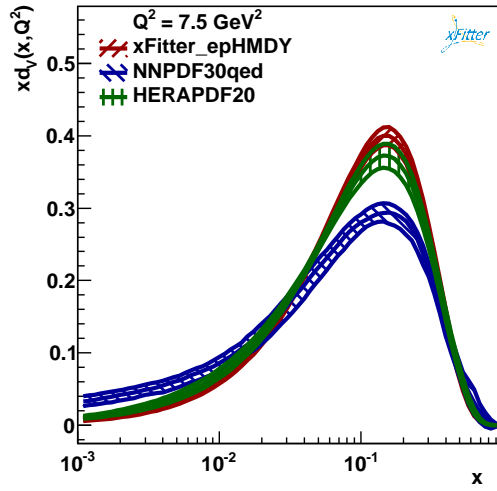
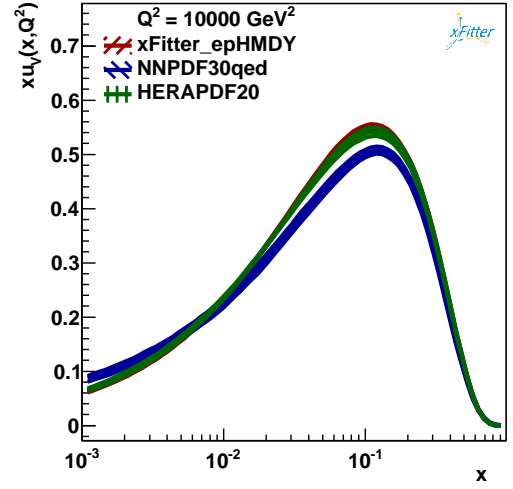
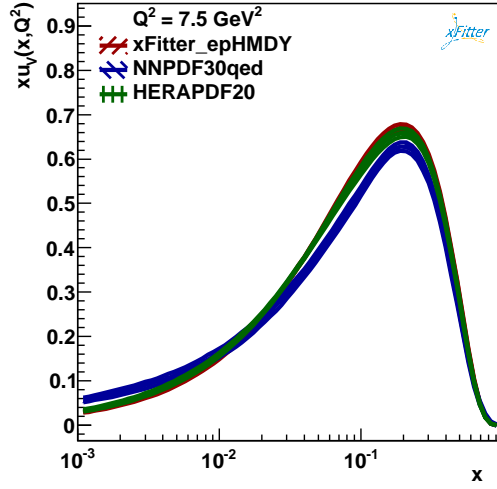
The parametrisation for HERA data differs from that of the HERAPDF2.0 PDF since the starting scale Q_0^2 is higher and the additional negative term in the gluon parametrisation is not necessary. Parametrisation and model uncertainties are considered according to the HERAPDF procedure [?] by adding extra terms which make little difference to the χ^2 of the fit, but which can change the shape of the PDFs. Additional parameters considered are: the extra negative term for the gluon; D_{u_v} , $D_{\bar{u}}$ and $E_{\bar{d}}$. Model variations considered are the variation of: m_b from 4.25 to 4.75 GeV; m_c from 1.41 to 1.53 GeV; Q_0^2 up to 10 GeV²; Q_{cut}^2 up to 10 GeV²; the strangeness fraction down to $f_s = 0.4$; the value of $\alpha_s(M_Z)$ from 0.116 to 0.120.

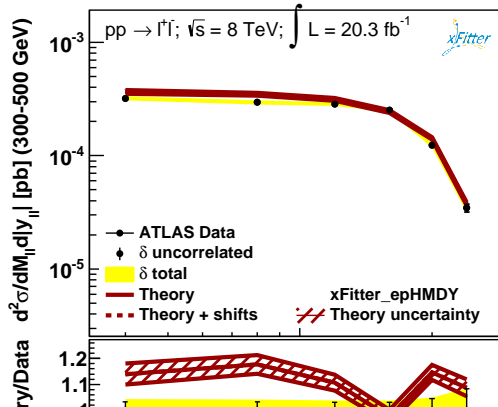
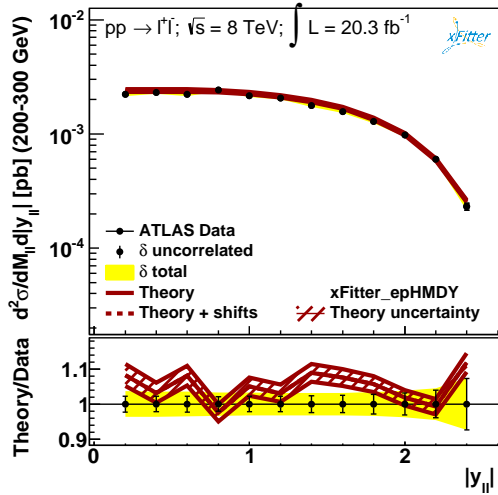
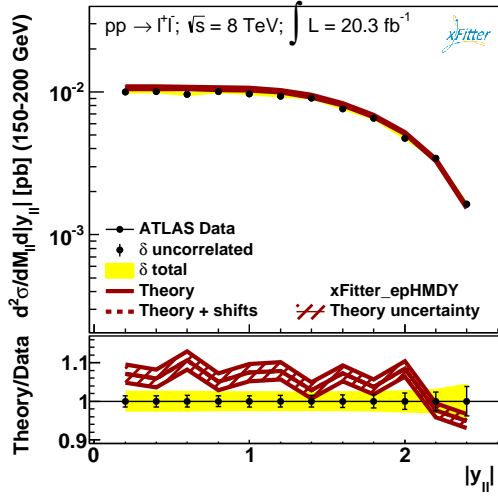
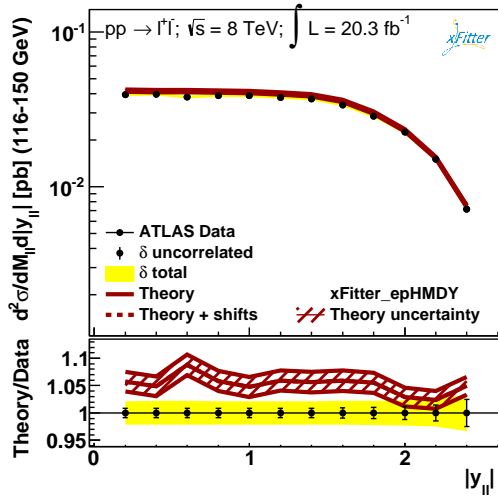
Fig. 1 shows the PDF distributions $xu_v, xd_v, x\bar{u}, x\bar{d}, xg$ at $Q^2 = 7.5^2 \text{ GeV}^2$, including model and parametrisation uncertainties, while Fig. 2 shows them at $Q^2 = 10^4 \text{ GeV}^2$. *Add model and parametrisation variations, Use NNLO MC central.* In these figures comparisons are made to the NNPDF3.0PDF set and the HERAPDF2.0 set. The shape of the xd_{u_v} distribution is close to that of HERAPDF2.0 because of the dominance of HERA data in the fit.

Fig. 3 shows the comparison between the high-mass Drell-Yan double differential distribution and the predictions. The χ^2 values for the high-mass Drell Yan data and the output parameters from NNLO fit can be found in Table. 4 and Table. 5 respectively.

The NNLO photon PDF distribution is shown both at the starting scale (7.5 GeV^2) and at 10^4 GeV^2 in Fig. 6, where it is also compared to an NLO extraction of the photon distribution. The x -range of the figure is restricted to the range of sensitivity of the high-mass drell-Yan data; $0.045 < x < 0.35$. The NLO and NNLO photon PDFs are compatible over this range.

Fig. 7 shows the photon distribution in the restricted range compared to the NNPDF3.0qed NNLO photon PDF. The uncertainties are considerably reduced. The comparison is shown at scale 100 GeV^2 and at 10^4 GeV^2 , where the value of 100 GeV^2 is chosen such that comparisons can also be made to the LUXqed [?] photon PDF, which is only defined above this scale. The HKR photon PDF [?] is also shown in this figure. The fit predictions from the present analysis agree with the LUXqed and the HKR photon PDFs at the 1- σ level.





| Dataset | xFitter_epHMDY |
|----------------------|----------------|
| HMDY rap 116-150 | 9.3 / |
| HMDY rap 150 200 | 17 / |
| HMDY rap 200 300 | 15 / |
| HMDY rap 300 500 | 3.8 / |
| HMDY rap 500 1500 | 4.2 / |
| Correlated χ^2 | 4.98 |
| Logpenalty χ^2 | -3.6 |
| Total χ^2 / dof | 55 / |
| χ^2 p-value | 0.01 |

Figure 4. χ^2 for high-mass Drell Yan data, for the NNLO fit

IV. CONCLUSIONS

| Parameter | xFitter epHMDY |
|---------------|-------------------------------|
| 'Bg' | $-0.220^{+0.014}_{-0.013}$ |
| 'Cg' | $6.92^{+0.62}_{-0.61}$ |
| 'Buv' | $0.761^{+0.017}_{-0.015}$ |
| 'Cuv' | $5.060^{+0.064}_{-0.092}$ |
| 'Euv' | $8.07^{+0.80}_{-0.82}$ |
| 'Bdv' | $1.009^{+0.050}_{-0.056}$ |
| 'Cdv' | $5.61^{+0.24}_{-0.30}$ |
| 'Cubar' | $6.37^{+0.56}_{-0.38}$ |
| 'Adbar' | $0.3226^{+0.0078}_{-0.0083}$ |
| 'Bdbar' | $-0.1921^{+0.0033}_{-0.0033}$ |
| 'Cdbar' | $14.0^{+2.0}_{-1.7}$ |
| 'alphas' | 0.1180 |
| 'rs' | 1.0000 |
| 'Aph' | $0.00120^{+0.031}_{-0.00089}$ |
| 'Bph' | $-0.62^{+0.63}_{-0.36}$ |
| 'Cph' | $10.0^{+13}_{-5.9}$ |
| 'Dph' | -4^{+210}_{-15} |
| 'Eph' | 87^{+257}_{-140} |
| Fit status | MC-replica |
| Uncertainties | median \pm 68cl |

Figure 5. PDF parameters for the NNLO fit.

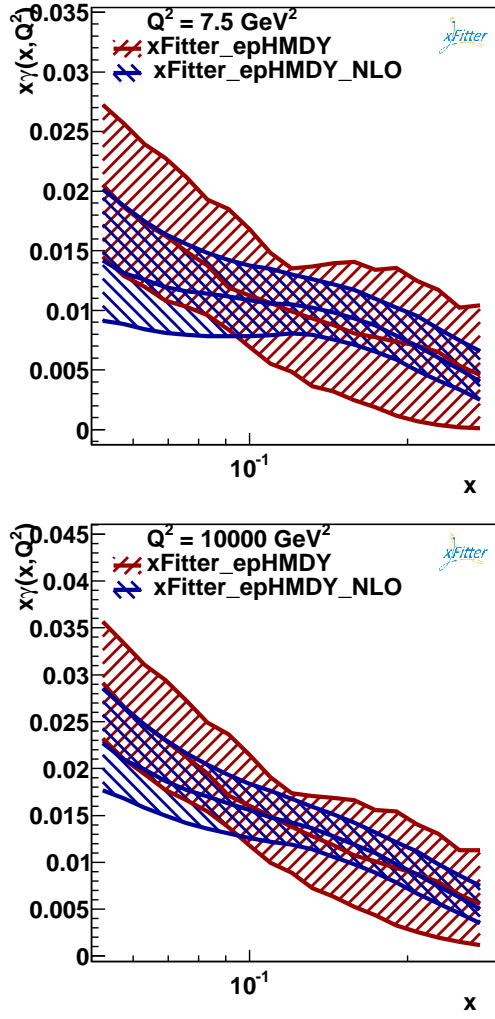


Figure 6. Comparison between the photon PDF distributions at NNLO and NLO: (a) at the starting scale; (b) at the evolved scale.

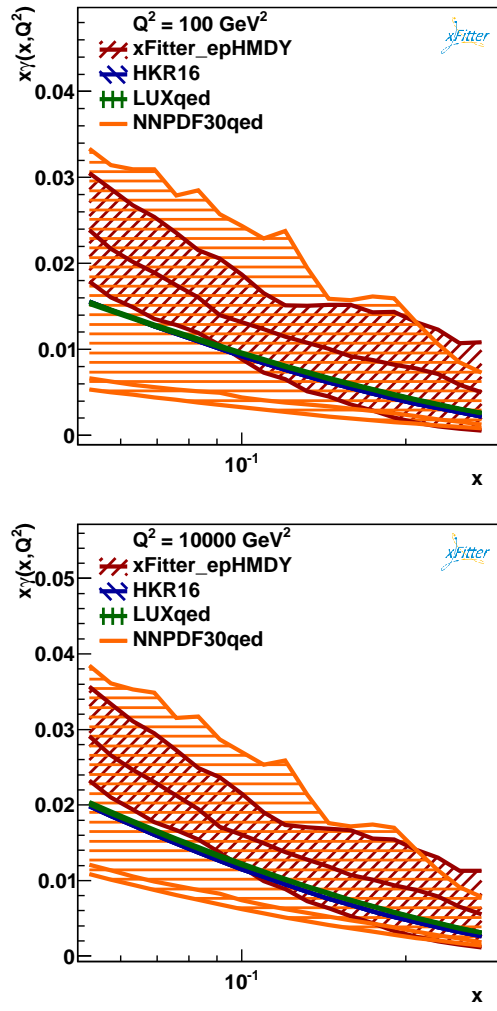


Figure 7. Comparison between the NNLO photon PDF distributions for the present analysis, NNPDF3.0QED, LUXqed, HKR: (a) at scale 100 GeV^2 ; (b) at the evolved scale 10000 GeV^2 .